Development 136, 739-747 (2009) doi:10.1242/dev.027904

FGF ligands in *Drosophila* have distinct activities required to support cell migration and differentiation

Snehalata Kadam, Amy McMahon, Phoebe Tzou and Angelike Stathopoulos*

Fibroblast growth factor (FGF) signaling controls a vast array of biological processes including cell differentiation and migration, wound healing and malignancy. In vertebrates, FGF signaling is complex, with over 100 predicted FGF ligand-receptor combinations. *Drosophila melanogaster* presents a simpler model system in which to study FGF signaling, with only three ligands and two FGF receptors (FGFRs) identified. Here we analyze the specificity of FGFR [Heartless (Htl) and Breathless (Btl)] activation by each of the FGF ligands [Pyramus (Pyr), Thisbe (Ths) and Branchless (Bnl)] in *Drosophila*. We confirm that both Pyr and Ths can activate Htl, and that only Bnl can activate Btl. To examine the role of each ligand in supporting activation of the Htl FGFR, we utilize genetic approaches that focus on the earliest stages of embryonic development. When *pyr* and *ths* are equivalently expressed using the Gal4 system, these ligands support qualitatively different FGFR signaling responses. Both Pyr and Ths function in a non-autonomous fashion to support mesoderm spreading during gastrulation, but Pyr exhibits a longer functional range. *pyr* and *ths* single mutants exhibit defects in mesoderm spreading during gastrulation, yet only *pyr* mutants exhibit severe defects in dorsal mesoderm specification. We demonstrate that the *Drosophila* FGFs have different activities and that cell migration and differentiation have different ligand requirements. Furthermore, these FGF ligands are not regulated solely by differential expression, but the sequences of these linked genes have evolved to serve different functions. We contend that inherent properties of FGF ligands make them suitable to support specific FGF-dependent processes, and that FGF ligands are not always interchangeable.

KEY WORDS: Cell migration and differentiation, *Drosophila*, FGF signaling, Ligand-receptor interactions

INTRODUCTION

Most Fibroblast growth factors (FGFs) have N-terminal signal peptides and are secreted from cells, allowing binding to and activation of their cell surface receptors (FGFRs). Studies in vertebrates, as well as simpler invertebrate model systems, have yielded valuable insights into the functions of this important gene family in multiple biological processes (Huang and Stern, 2005; Rottinger et al., 2008; Thisse and Thisse, 2005). In embryos, these functions include mesoderm induction and patterning, cell growth, migration and differentiation. Later functions include organ formation and maintenance, neuronal differentiation and survival, wound healing and malignant transformation (Chen and Deng, 2005; Coumoul and Deng, 2003; Eswarakumar et al., 2005). FGFs often signal directionally across epithelial-mesenchymal boundaries and exhibit diverse and dynamic patterns of expression that are both spatially and temporally restricted. Tightly regulated expression is one mechanism that helps to ensure the specificity of FGF signaling through FGFRs. An additional level of specificity is most likely imparted by their divergent amino acid sequences, resulting in differential binding affinity for the FGFR, heparan sulfate proteoglycan (HSPG)-interaction specificity (a co-factor involved in FGF-FGFR interaction), and/or FGF ligand range of action (e.g. diffusibility).

FGF and FGFR genes have been identified in organisms ranging from the nematode and fly to mouse and human. There are two FGFs and one FGFR in *Caenorhabditis elegans*, and three FGFs and two FGFRs in *Drosophila melanogaster*, as compared with 24 FGFs and four FGFRs (three of which exhibit alternative splicing) in humans and mice (Birnbaum et al., 2005; Huang and Stern, 2005). In vertebrates, over 100 potential FGF-FGFR complexes are predicted (Zhang et al., 2006). Thus, the expectation is that with so many combinations possible, tight regulation of FGF activity and receptor specificity must exist to regulate signaling. Many FGF-FGFR interactions have been studied in the vertebrate system, but the genetic redundancy can make dissection of the functional contribution of particular FGF-FGFR interactions challenging (e.g. Mariani et al., 2008). Often, more than four ligands interact with a particular FGFR isoform at any one time.

Drosophila is an excellent model system for studying FGF signaling, especially now that it appears that the full repertoire of FGF ligands and receptors has been identified (reviewed by Huang and Stern, 2005). Relatively few FGF-FGFR interactions are possible, with only three FGF ligands [Pyramus (Pyr), Thisbe (Ths) and Branchless (Bnl)] and two FGF receptors [Heartless (Htl) and Breathless (Btl)] (reviewed by Ornitz and Itoh, 2001; Szebenyi and Fallon, 1999). The FGFR Btl, and its FGF ligand Bnl, control tracheal branching in the embryo, mesoderm migration over male genital discs, and air sac formation in the larva (Ahmad and Baker, 2002; Sato and Kornberg, 2002; Sutherland et al., 1996). The preliminary function of the Htl FGFR is to control mesoderm migration during gastrulation (Beiman et al., 1996; Gisselbrecht et al., 1996; Shishido et al., 1997). Later in development, among other functions, Htl is also required for the differentiation of cells that form the heart and hindgut musculature (Michelson et al., 1998; San Martin and Bate, 2001). The ligands for the Htl FGFR in *Drosophila* had remained elusive, until *pyr* and *ths* were identified by genomic screens (Stathopoulos et al., 2004; Gryzik and Muller, 2004). Pyr and Ths share homology with the FGF8 family of vertebrate FGFs. Genetic evidence suggests that this pair of invertebrate FGFs functions through a single FGFR, Htl, to control cell migration and differentiation, as a deficiency mutant that removes both ligands phenocopies the *htl* mutant (Stathopoulos et al., 2004; Gryzik and

California Institute of Technology, Division of Biology MC114-96, 1200 East California Boulevard, Pasadena, CA 91125, USA.

*Author for correspondence (e-mail: angelike@caltech.edu)

Accepted 30 December 2008

Muller, 2004). Thus, *Drosophila melanogaster* provides a unique opportunity within an invertebrate model system, amenable to genetic approaches, to gain insights into why multiple FGF ligands are utilized to activate the same receptor isoform, as is typically the case in vertebrates.

A question in the FGF field is whether the specificity of receptor-ligand interactions is accomplished through the differential expression of ligands or through differences in the signaling properties of the ligand proteins themselves. An impressive analysis of all vertebrate FGF-FGFR interactions was recently completed, in which the binding specificities of ligand-receptor interactions were examined in tissue culture (Ornitz et al., 1996; Zhang et al., 2006). Specificity of receptor-ligand interactions was demonstrated in this system; however, how this relates to in vivo processes is, for the most part, undetermined. Only a limited number of in vivo studies have been conducted to analyze the function of particular FGF-FGFR interactions (e.g. Rentzsch et al., 2008; Yang et al., 2002). In this study, we examine the individual functions of the FGF ligands Pyr and Ths in *Drosophila* in order to define whether these ligands have distinct functions and/or function redundantly, and to gain insights into why multiple ligands are typically involved in activating a particular FGFR coordinately. We find that the regulated expression of ligands and their divergent protein sequence both contribute to the specificity of FGF-FGFR interactions.

MATERIALS AND METHODS

Fly stocks and genetic approaches

Unless otherwise noted, fly stocks were obtained from the Bloomington Stock Center and were reared under standard conditions at 25°C. The genotype 'wild type' refers to the *yw* genetic background. *Df(2R)BSC25* has been described (Stathopoulos et al., 2004). The Gal4 drivers *zenVRE.Kr*-Gal4 and *sim*-Gal4 were obtained from M. Frasch (University of Erlangen-Nuremberg, Germany) and Stephen Crews (University of North Carolina, Chapel Hill, NC, USA), respectively. Two PiggyBac insertion stocks were obtained from the Exelixis Collection Stock Center at Harvard Medical School (Thibault et al., 2004); we determined that P02915 is located in the first intron of *pyr*, and confirmed that P02026 is located in the second intron of *ths*.

Df(2R)ths238 is a deletion of the *ths* gene that was created in the course of this study through a genetic screen for male-specific recombination (see Preston et al., 1996) using P9.1.2, a viable P-element insertion located ~400 bp upstream from the *ths* transcription start site, as mapped by RACE (see Fig. 2A). Line P9.1.2 resulted from mobilization of P10004, a viable insertion located ~900 bp upstream from the *ths* transcription start site, to remove 500 bp of *ths* upstream sequence. Deletion breakpoints were confirmed using inverse PCR, in the case that the P-element was retained [i.e. *Df(2R)BSC25* and *Df(2R)ths238*].

Df(2R)pyr36 is a deletion of the *pyr* gene that was created by mobilization of the P9.1.2 insertion and screening for excision events. The breakpoints of this deficiency were mapped by complementation using available zygotic lethal insertions (including wal^{EY09961} and wal^{k14026}); we contend that the *Df(2R)pyr36* does not extend past the *walrus* (*wal*) and *ths* genes. The 500 bp of *ths* upstream sequence that was removed in the creation of line P9.1.2 is also absent from *Df(2R)pyr36*. Yet, *ths* transcript levels and domains of expression appear similar to those of the wild type in *Df(2R)pyr36*/*Df(2R)pyr36* mutant embryos (expression up to stage 15 was examined; see Fig. 2F and data not shown). It is formally possible that cis-regulatory sequences controlling expression at later stages were removed. However, as the phenotypes exhibited by *Df(2R)pyr36* are subtle relative to *Df(2R)BSC25*, and as the FGF-homologous portion of Ths is located at its N-terminus, it is likely that *Df(2R)pyr36* does not remove *ths* coding sequence.

UAS-*bnl* and UAS-*ths* have been described previously (Stathopoulos et al., 2004; Sutherland et al., 1996). UAS-*pyr* was generated during the course of this work. No EST is available for *pyr*. Therefore, the 5′ and 3′ ends of the *pyr* gene were determined by RACE (Stathopoulos et al., 2004). Primers based on this sequence were used to PCR amplify the intact *pyr* gene. PCR of the intact full-length gene from the RACE cDNA with a single primer pair was not possible, probably owing to repeats within the gene. Instead, two separate PCR reactions were performed to isolate sequence spanning the full-length gene (one to amplify the 5′ end from cDNA and the other to obtain sequence corresponding to the last exon from genomic DNA). The two products were ligated in a three-way ligation to reconstitute the full-length *pyr* coding sequence.

UAS-*pyr* and UAS-*ths* fly stocks were constructed using standard methods (Spralding and Rubin, 1982). For the genetic rescue experiments, virgins of the following genetic backgrounds (#1) *Df(2R)BSC25 sim-Gal4/CyO ftz-lacZ*, (#2) *Df(2R)BSC25/CyO wg-lacZ*; *zenVRE.Kr-Gal4* and (#3) *Df(2R)BSC25/CyO wg-lacZ*; *69B-Gal4* were crossed with males from (#4) *Df(2R)BSC25*/*CyO wg-lacZ*; *UAS-pyr*, (#5) *Df(2R)BSC25*/*CyO wg-lacZ*; *UAS-ths*, (#6) *Df(2R)BSC25*/*CyO wg-lacZ*; *UAS-bnl*, (#7) *Df(2R)BSC25/CyO ftz-lacZ*; *UAS-pyr*, (#8) *Df(2R)BSC25/CyO ftz-lacZ*; *UAS-ths* or (#9) *Df(2R)BSC25/CyO ftz-lacZ*; *UAS-bnl*.

Quantitative PCR

Embryos were manually separated and flash frozen using liquid nitrogen. Three biological replicates of each sample (i.e. 20 dechorionated embryos of stage 9/10) were obtained. Total RNA isolation was carried out using the RNeasy Micro Kit (Qiagen) and quantified using a ND-1000 spectrophotometer (NanoDrop Technologies). One microgram of total RNA was used for reverse transcription to synthesize cDNA using the Gene Racer Superscript III RT Module Kit (Invitrogen). The quantitative PCR (qPCR) reaction was performed in 96-well format using LightCycler SYBR Green 480 (Roche). The qPCR was set up as follows: 95°C for 5 minutes; 35 cycles of 95°C for 20 seconds, 55°C for 20 seconds, and 72°C for 30 seconds; and a final 72°C for 10 minutes. For quantifying the transcript levels in ectopically expressing *pyr* and *ths* lines, the data were normalized to the transcript level of a housekeeping gene, *Elongation factor 1* (Ishimoto et al., 2005). In order to quantify the levels of 'ectopic' *pyr* and *ths* expression supported by the Gal4 driver and transgenes containing UAS, we used *twist*-Gal4 and UASlacZ as a control and subtracted the endogenous *pyr* and *ths* transcript levels; the domain of ectopic expression supported by *twist*-Gal4 is significant, as compared with expression supported by *zenVRE.Kr*-Gal4 and *sim*-Gal4, and thereby allowed for better resolution of the levels of ectopic expression.

The lines chosen [*pyr*line1: UAS-pyr:AMS330(III) and *ths*line1: UAS-ths:AMS289.22(III)] exhibit comparable levels of ectopic expression as assayed by qPCR (see Fig. S4 in the supplementary material) and support equivalent Eve^{+} expression when driven by *69B*-Gal4 (see Fig. S3D,E in the supplementary material). In another set of insertions, approximately twice as much ectopic *ths* was supported, relative to the levels of *pyr* (see Fig. S4 in the supplementary material, *ths*line2 and *pyr*line2); nevertheless, the same results were obtained with this other set of lines in the *zenVRE.Kr*-Gal4-driven rescue experiments (data not shown). Therefore, we contend that the ability of *pyr* alone to support the migration of mesoderm cells at a distance is not due to differences in expression levels resulting from positional effects on transgene expression.

Immunohistochemistry, in situ hybridization and sectioning

The following antibodies were used: guinea pig anti-Twist (1:200; from M. Levine, UC Berkeley, CA, USA), mouse anti-dpERK (1:200; Sigma), rabbit anti-β-galactosidase (1:200; Molecular Probes), rabbit anti-Eve (1:400; from M. Frasch) and monoclonal 2A12 (1:3; Developmental Studies Hybridoma Bank). In situ hybridization (Kosman et al., 2004; Lehmann and Tautz, 1994), double antibody plus in situ hybridization detection of protein and transcript levels (Frasch, 1995), and staining of tracheal branches using 2A12 antibody (Sutherland et al., 1996) were conducted as previously described.

For sectioning, embryos were sorted for appropriate stage and genotype (i.e. using balancer chromosomes containing reporters), and embedded in acetone-Araldite (Electron Microscopy Sciences) as described (Leptin and Grunewald, 1990). Sections (10 μm) were cut using a Historange 2218 microtome.

Because variability is present in the *Df(2R)BSC25* mutant background, a system of quantitation of mutant phenotype was devised. We scored mesoderm spreading phenotypes in the deficiency and the ectopically

expressing lines (see Figs S5 and S6 in the supplementary material). Clumping was used as a measure of the ability of ligands to attract cells to the ventral midline; the multilayer phenotype was scored by assessing the ability of ligands to attract cells to the dorsal-most ectoderm.

RESULTS

pyr and *ths* are dynamically expressed within *Drosophila* embryos

It is likely that Pyr and Ths are ligands for the Htl FGF receptor, as these genes are expressed near sites of Htl expression (Stathopoulos et al., 2004). During gastrulation, *pyr* and *ths* are expressed in distinct domains within the ectoderm at the surface of the embryo (see Fig. 1A-C). Early in development, *ths* is expressed in ventral regions (Fig. 1F,G) and *pyr* is expressed in dorsal regions (Fig. 1D,E). Once invagination is complete and all mesoderm cells have entered the interior of the embryo, these cells proceed to migrate along the inner ectodermal surface, forming a monolayer. Activation of the FGFR Htl is thought to trigger the spreading of the mesoderm across the underlying ectoderm (Fig. 1A). The dynamic expression domains of the ligands suggested a possible mechanism by which directional information could be imparted to the mesoderm cells moving beneath, causing these cells to move in the dorsal direction.

Ligand choice and expression domain are important for FGF signaling

To determine whether the distinct domains of ligand expression are important for proper mesoderm migration, we altered their expression domains and assayed effects on mesoderm spreading. Using the *69B*-Gal4 driver, the *bnl*, *pyr* and *ths* FGF-encoding genes were ectopically expressed throughout the entire ectoderm (Fig. 1H-M). For *pyr* and *ths*, several transgenic lines were first compared with the control for positional effects that might influence the levels of gene expression, and a set of lines was chosen that exhibited comparable levels of ectopic expression by Gal4 as assayed by qPCR (see Fig. S4 in the supplementary material). Ectopic expression of Pyr throughout the ectoderm resulted in mesoderm migration defects (Fig. 1J,K; n=9). The *pyr* ectopic expression defect was specific; mesoderm spreading occurred, but a cell monolayer was not formed (Fig. 1K). By contrast, ectopic expression of Bnl or Ths in the same manner had little to no effect on mesoderm monolayer formation (Fig. 1G,I and Fig. 1L,M; n=6 and n=10, respectively).

The MAPK pathway is activated in migrating mesodermal cells as a result of FGFR receptor tyrosine kinase activation, and leads to dual phosphorylation of MAPK [also known as ERK (Gabay et al., 1997) and Rolled – FlyBase]. A monoclonal antibody that recognizes this activated form of MAPK (dpERK) can be used to monitor activation of this pathway within cells. dpERK staining is observed within gastrulating embryos at the leading edge of the migrating mesoderm cells (see Fig. S1A in the supplementary material), but is lost in the absence of Htl activation (Michelson et al., 1998; Stathopoulos et al., 2004). In embryos ectopically expressing *pyr* or *ths* via *twist*-Gal4, which supports their expression throughout the mesoderm, dpERK is ectopically expressed throughout all mesoderm cells (see Fig. S1C,E in the supplementary material) (Stathopoulos et al., 2004). However, when the *69B*-Gal4 driver was used to ectopically express *pyr* or *ths*, only the ectopic expression of *pyr* supported ectopic activation of ERK throughout the entire mesoderm (compare Fig. S1D with Fig. S1F in the supplementary material). Ectopic expression of *bnl* had no effect: dpERK remained localized at the leading edge of the migrating mesoderm [compare Fig. S1B with Fig. S1A (see arrowheads) in the supplementary material]. Depending on where the ligands were expressed, differences in the capacity of Pyr versus Ths to activate signaling were observed, whereas Bnl had no effect. Furthermore, the ability of these ligands to support ectopic dpERK expression was found to correlate with the inhibition of mesoderm migration (see Fig. 1; data not shown).

We then assayed the ability of Pyr and Ths to influence trachea formation, a function that is supported by Bnl-Btl. Ectopic expression of *bnl* via *69B*-Gal4 leads to a substantial increase in tracheal branching (compare Fig. S2B with Fig. S2A in the supplementary material) (Sutherland et al., 1996). However, no such effect on the trachea was observed upon ectopic expression of *pyr* or *ths* (see Fig. S2C,D in the supplementary material), suggesting that neither Pyr nor Ths can activate the Btl FGFR.

Isolation and initial characterization of *pyr* and *ths* single mutants

Mesoderm spreading defects are observed in *htl* mutants and in a deficiency mutant, *Df(2R)BSC25*, that removes both *pyr* and *ths* (Fig. 2A) (Beiman et al., 1996; Gisselbrecht et al., 1996; Stathopoulos et al., 2004). We sought to test further the requirement for Pyr or Ths in activation of the Htl FGFR by analysis of single-

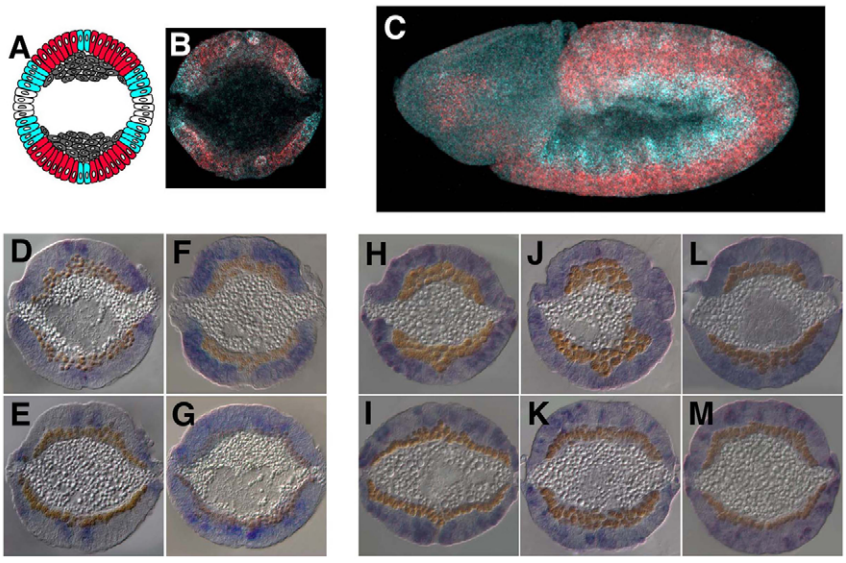

Fig. 1. Dynamic expression patterns of *pyr* and *ths* regulate mesoderm migration. (A,B,D-M) *Drosophila* embryo cross-sections; (A-C,D,F,H,J,L) stage 8 embryos; (E,G,I,K,M) stage 9/10 embryos. (C) Whole-mount embryo oriented with anterior to the left and dorsal up. (**A**) Schematic representation of a stage 8 embryo in cross-section depicting expression patterns of *pyr* (blue) and *ths* (red). (**B**,**C**) During gastrulation, *pyr* (blue) and *ths* (red) are expressed in distinct domains of the neurogenic ectoderm at the surface of the developing embryo, concurrent with spreading of mesoderm cells within the interior of the embryo. (**D-G**) Endogeneous *pyr* (D,E) and *ths* (F,G) expression patterns (blue). (**H-M**) Ectopic expression of *bnl* (H,I), *pyr* (J,K), *ths* (L,M) in the ectoderm using the *69B*-Gal4 driver (blue).

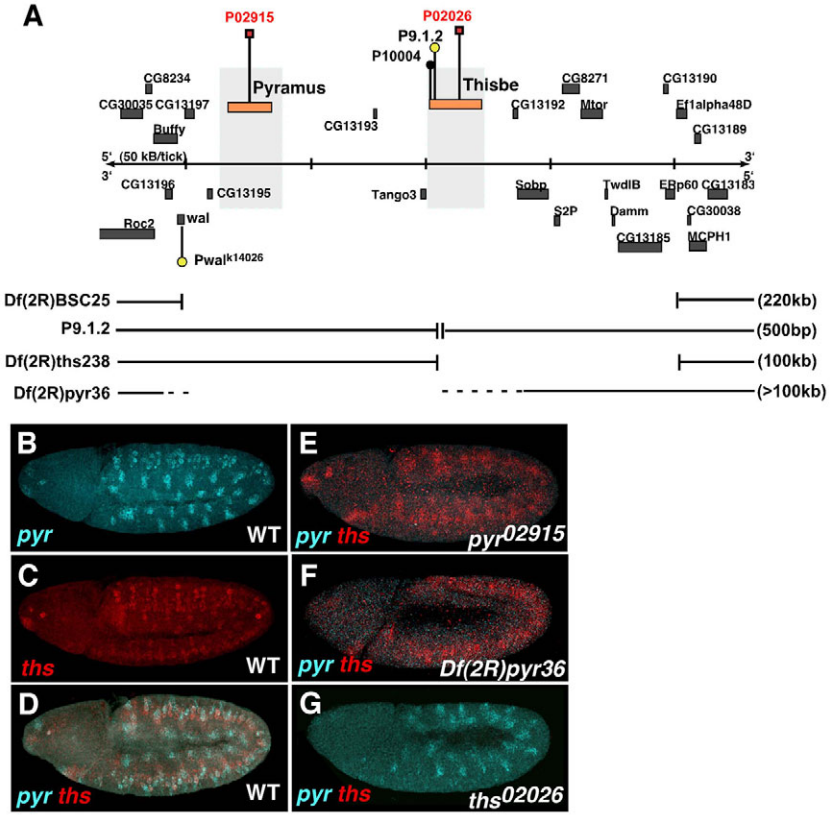

Fig. 2. Summary of *pyr* and *ths* single-mutant isolation: genetic alleles and expression analysis. (**A**) The genomic region containing the *Drosophila pyr* and *ths* loci, and P-element/PiggyBac insertions and deficiencies identified in this area. *Df(2R)BSC25* deletes ~220 kb (Stathopoulos et al., 2004). P9.1.2 deletes ~500 bp located ~400 bp upstream of the *ths* promoter, and was achieved through a male-specific recombination screen using the P10004 insertion. *Df(2R)ths238* deletes ~100 kb including the entire *ths* coding sequence. *Df(2R)pyr36* removes ~100 kb, including the entire *pyr* coding sequence. (**B-G**) Double in situ hybridization using riboprobes to detect expression of both *pyr* (blue) and *ths* (red) transcripts within embryos at stage 10. Embryos are oriented with anterior to the left and dorsal up. Co-expression patterns are depicted in wild-type embryos (B-D). In pyr^{02915} (E) and *Df(2R)pyr36* (F) mutant embryos, no *pyr* expression is detected, yet *ths* expression appears normal. In ths^{02026} mutant embryos, no *ths* expression is detected, yet the *pyr* expression domain appears normal (G).

mutant phenotypes. First, we identified two PiggyBac insertions located in proximity to *pyr* and *ths* (see Fig. 2A). The line containing the *pyr* insertion, pyr^{02915}, is zygotically lethal, whereas the line containing the *ths* insertion, ths^{02026}, is only semi-lethal [i.e. homozygous flies are obtained at very low frequencies (~0.5%) and are short-lived]. Each insertion disrupts expression of the respective gene, and we detect no effect on expression of the other ligand (see Fig. 2E,G, compare with Fig. 2A-C). As phenotypes associated with insertions can vary, we chose to identify true null alleles.

Deletions of the entire *pyr* or *ths* coding sequences were created (see Fig. 2A and Materials and methods). Because *pyr* and *ths* are linked, deletions resulting from mobilization of the insertion P10004 had the potential to remove either *ths* or *pyr* sequences. Through several rounds of male-specific recombination screening, we were able to identify a deletion that removes the *ths* gene in its entirety, which we named *Df(2R)ths238*. The entire *ths* coding sequence, as well as ten proximal genes, are absent, yet the entire *pyr* locus remains intact. Using excision-based screening with the same P9.1.2 insertion, we obtained a deletion that removes sequence upstream of *ths*, including the entire *pyr* gene and five proximal genes, which we named *Df(2R)pyr36*.

Complementation tests were conducted to determine genetic interactions between our allelic series of *pyr* and *ths* mutants. We believe that the pyr^{02915} allele represents a *pyr* null, as no expression of *pyr* was detected at any time-point examined. It is unclear whether the ths^{02026} allele represents a *ths* null, as expression could be detected in the visceral mesoderm at later stages (data not shown). *Df(2R)pyr36* and *Df(2R)ths238* represent null alleles of *pyr* and *ths*, respectively, because the entire coding region of each gene is absent; however, of note is the fact that other genes are also removed by these ~100 kb deletions (see Materials and methods for details). This allelic series (i.e. PiggyBac insertions: weak alleles; *Df(2R)pyr36* and *Df(2R)ths238* deficiencies: strong alleles; *Df(2R)BSC25* deficiency: double mutant; see Fig. 2A) provided the first opportunity to analyze transheterozygous combinations in order to gain insights into *pyr* and *ths* single-mutant phenotypes. In both *pyr* and *ths* single mutants, the mesoderm spreading was aberrant (Fig. 3G-J, compare with Fig. 3A,B). The mesoderm was multilayered and a monolayer rarely formed. However, neither mutant exhibited a phenotype as severe as that of the *Df(2R)BSC25* or *htl* mutants (Fig. 3C-F), suggesting a role for both Pyr and Ths in guiding mesoderm spreading.

Importance of positional information in the function of ligands during mesoderm spreading

To determine whether the localized expression of each ligand is important for its function, we took an ectopic expression approach using Gal4 to promote expression of a given ligand in the *pyr* and *ths* double-mutant background. *Df(2R)BSC25* removes both *pyr* and *ths*, and 16 other genes, none of which has known embryonic phenotypes (Fig. 2A) (Stathopoulos et al., 2004). The *sim*-Gal4 driver (Xiao et al., 1996) delivers ligands at the ventral midline where *single-minded* (*sim*) is normally expressed (see Fig. 4F). Alternatively, the *zenVRE.Kr*-Gal4 driver can be used to deliver ligands to the dorsal domain of the ectoderm within the lower half of gastrulating embryos (see Fig. 4K) (Frasch, 1995).

When the *sim*-Gal4 driver was used to express either *pyr* or *ths* in the *Df(2R)BSC25* mutant background (Fig. 4F), no rescue of mesoderm spreading was observed (Fig. 4G,H). In fact, clumps of mesoderm cells were observed overlying the site of Pyr ectopic expression, suggesting that this ligand had attracted mesoderm cells to this position (Fig. 4G). This phenotype appeared to be more severe than that of *Df(2R)BSC25* mutants (Fig. 4G,H, compare with Fig. 4B,C; see Fig. S5 in the supplementary material; $P<0.01$). Ectopic expression of *ths* in this manner also had a weak effect, as

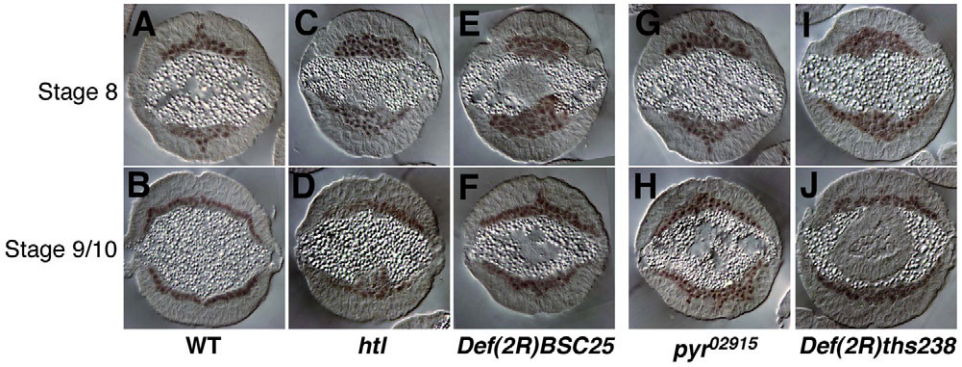

Fig. 3. Pyr and Ths are both required for normal mesoderm spreading. *Drosophila* embryos were stained with anti-Twist antibody and sectioned as described (see Materials and methods). (A,B) Wild-type embryos; (C,D) htl^{AB42} mutant; (E,F) *Df(2R)BSC25* mutant, which lacks both *pyr* and *ths*; (G,H) *pyr* single mutant (pyr^{02915}/pyr^{02915}); (I,J) *ths* single mutant [*Df(2R)ths238/Df(2R)ths238*]. (**A**,**B**) In wild-type embryos at stage 8, the invaginated tube collapses and the mesodermal cells start migrating (A). At stage 9/10, the spreading of the mesoderm is complete, resulting in the formation of a single layer along the internal surface of the ectoderm (B). (**C-J**) In mutants, the invaginated tube appears to have collapsed normally at stage 8 (C,E,G,I), but the mesoderm cells exhibit spreading defects that present as a multilayered phenotype at stage 9-10 (D,F,H,J). Cells do not appear to migrate toward dorsal regions and a monolayer is not formed.

cells tended to pool at the ventral midline (Fig. 4H), but this effect was not supported by statistical significance as the *Df(2R)BSC25* mutants themselves exhibit variability (Fig. 4B,C and see Fig. S5 in the supplementary material).

Different results were obtained using the *zenVRE.Kr*-Gal4 driver. In this case, ectopic expression of either *pyr* or *ths* did appear sufficient to direct mesoderm cells toward dorsal regions of the ectoderm in the lower ventral half of *Df(2R)BSC25* mutant embryos (Fig. 4L,M; n=17 and n=19, respectively), within the domain of ectopic expression supported by the driver (see Fig. 4K). In *Df(2R)BSC25* mutant embryos, some spreading toward dorsal regions was observed in only 28% of the embryos examined (n=10 of 36 embryos scored in total) (Fig. 4B and see Fig. S5 in the supplementary material); therefore, this 'rescue' in the lower half of the embryos by *pyr* and *ths* is significant (see Figs S5 and S6 in the supplementary material). Surprisingly, however, ectopic expression of *pyr* in this manner was also capable of directing the movement of mesoderm cells in the top half of embryos, at a distance from the source of *pyr* expression supported by *zenVRE.Kr*-Gal4. For *ths* ectopic expression, the effect on the top half was not as strong and exhibited more variability (see Figs S5 and S6

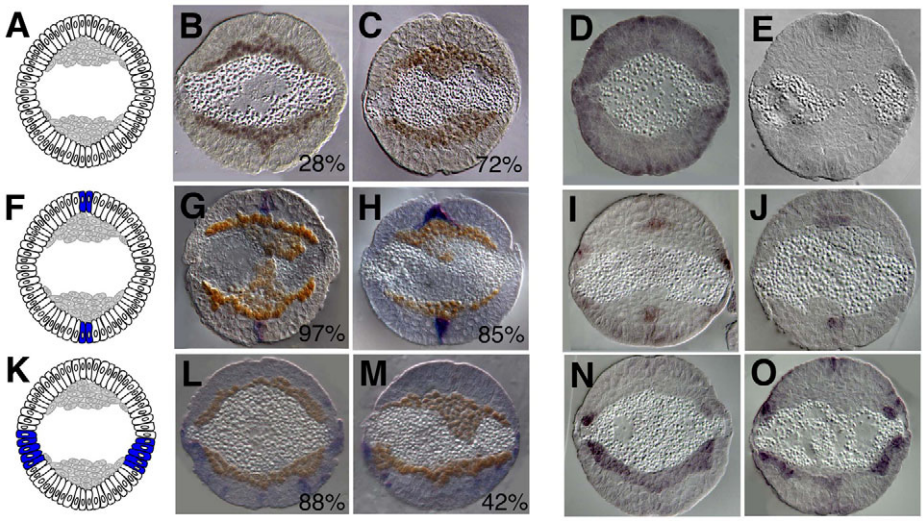

Fig. 4. The specific expression domain of *pyr* is required for normal mesoderm spreading. (B,C,G,H,L,M) *Drosophila* embryos stained with anti-Twist antibody (brown) to detect mesoderm cells and hybridized with the specified riboprobes by in situ hybridization to detect transcripts (blue); the percentage of embryos exhibiting the mutant phenotype shown is indicated. (D,E,I,J,N,O) Embryos stained with anti-dpERK antibody. Cross-section views are of stage 9/10 embryos. (**A**) Schematic of a *Df(2R)BSC25* mutant embryo in cross-section; no ectopic expression. (**B**,**C**) Variation in the phenotype of the *Df(2R)BSC25* mutant background. Often, spreading can occur, but monolayer formation is defective (B). Alternatively, neither spreading nor monolayer formation occurs (C). (**D**) dpERK staining is observed in the leading edge in the wild-type embryo (see arrowhead) (Gabay et al., 1997). (**E**) dpERK staining is absent in *Df(2R)BSC25* embryos (Stathopoulos et al., 2004). (**F**) Schematic of ectopic expression of either ligand (*pyr* or *ths*) in the ventral midline of *Df(2R)BSC25* mutants using the *sim*-Gal4 driver (Xiao et al., 1996). (**G-J**) Ectopic expression of *pyr* (G,I) or *ths* (H,J) in the ventral midline using *sim*-Gal4 in the *Df(2R)BSC25* mutant background. (**K**) Schematic of ectopic expression of either ligand within the dorsal ectoderm of *Df(2R)BSC25* mutants using the *zenVRE.Kr*-Gal4 driver (Frasch, 1995). (**L-O**) Ectopic expression of *pyr* (L,N) or *ths* (M,O) in the dorsal-lateral region of the ectoderm using *zenVRE.Kr*-Gal4 in the *Df(2R)BSC25* mutant background.

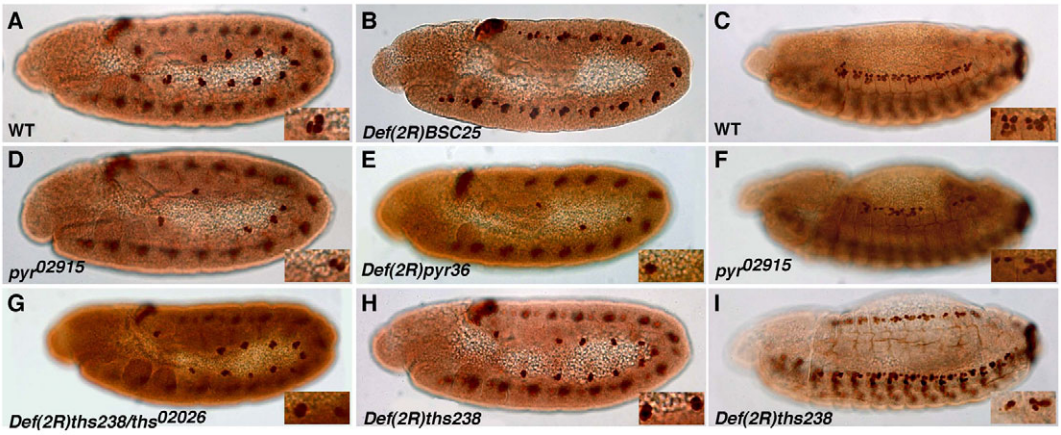

Fig. 5. The Pyr FGF ligand is necessary for the differentiation of dorsal mesoderm cell lineages. *Drosophila* embryos were stained with an anti-Eve antibody to examine specification of dorsal mesoderm lineages. Depicted are wild-type embryos at stage 11 (A) and stage 14 (C); *Df(2R)BSC25* mutant embryos, which lack both *pyr* and *ths* genes, at stage 11 (B); *pyr* single mutants at stage 11 (D,E) and stage 14 (F); and *ths* single mutants at stage 11 (G,H) and stage 14 (I). The insets display Eve$^+$ cell clusters at 10× magnification. (**A**,**C**) In wild-type embryos at stage 11 (A), there are 11 independent clusters of three Eve$^+$ cells each within the dorsal somatic mesoderm. At stage 14 (C), these join to form a continuous row of heart progenitors. (**B**) Eve$^+$ clusters are absent from the dorsal mesoderm of *Df(2R)BSC25* mutant embryos. (**D-F**) In both the weakest (*pyr*^{02915}/*pyr*^{02915}) and the strongest [*Df(2R)pyr36*/*Df(2R)pyr36*] alleles of *pyr* single mutants (D and E, respectively), the number of Eve$^+$ clusters is significantly reduced, resulting in gaps within the row of heart progenitors at stage 14 (F). (**G-I**) By contrast, within *ths* mutant embryos at stage 11, when either a weak mutant [*Df(2R)ths238*/*ths*^{02026}] or the strongest alleles [*Df(2R)ths238*/*Df(2R)ths238*] are examined (G and H, respectively), there are only subtle effects on Eve$^+$ cell specification (see inset; often two Eve$^+$ cells are present instead of three). At later stages, defects are more apparent (I).

in the supplementary material). In *Df(2R)BSC25*, as well as in *htl*^{AB42} mutants, such a 'mixed' phenotype was not typical, as both top and bottom halves of the embryo exhibited similar phenotypes (see Fig. 4L,M, compare with Fig. 4C).

Collectively, these results suggest that localized *pyr* expression is important to support mesoderm spreading, as *zenVRE.Kr*-Gal4 is able to promote spreading, whereas *sim*-Gal4 is not, and also suggest the hypothesis that Pyr protein can function at a distance, whereas Ths functions more locally. To test this, embryos were assayed for dpERK activity (Fig. 4D-O). Both *pyr* and *ths* expression through *sim*-Gal4 was able to support dpERK activation (Fig. 4I,J). Therefore, the weaker effect of *ths* is unlikely to be due to an inability to activate the receptor in this domain. Moreover, *pyr* expression through *zenVRE.Kr*-Gal4 supported strong activation of dpERK throughout the lower half of the embryos (Fig. 4N), whereas the effect of ectopic expression of *ths* in this same domain was more limited (Fig. 4O). Both *pyr* and *ths* expression supported dpERK activation at the leading edge of mesoderm cells in the top half of embryos (Fig. 4N,O). Mesoderm cells in the top half of the embryo are able to receive both Pyr and Ths signals, but only a subset of the cells migrates toward the dorsal ectoderm in response to Ths (see Discussion).

FGF ligand specificity during mesoderm differentiation

After mesoderm cell spreading has been completed, both Pyr and Ths are expressed in regions of the dorsal ectoderm that abut a subset of the mesoderm cells (Fig. 2D and see Fig. S3A,B in the supplementary material). *pyr* is present in more-dorsal regions of the ectoderm, overlying sites of dorsal mesoderm specification; limited expression of *ths* is also seen in this same region (Fig. 2D). The mesoderm cells that come into contact with the dorsal ectoderm receive an inductive signal from Decapentaplegic (Dpp), a *Drosophila* TGFβ homolog (reviewed by Frasch, 1999). Thereby, expression of genes such as *even skipped* (*eve*) and *tinman*, which are required for the differentiation of cardiac and pericardial tissues, depend on Dpp as well as on Htl-dependent FGF signaling.

We sought to define the role of each ligand in the specification of dorsal mesoderm cell lineages within germ-band elongated embryos. Normally, Eve is expressed within 12 hemisegments. In *pyr* single mutants, often only a few hemisegments exhibited Eve expression (Fig. 5D,E, compare with Fig. 5A), whereas within *ths* single-mutant embryos, only subtle defects in Eve$^+$ cell specification were observed (Fig. 5G,H, compare with Fig. 5A). The *pyr* mutant phenotype was much stronger than the phenotype exhibited by *ths* single mutants at all stages examined, and even when comparisons were made between the weakest *pyr* allele (*pyr*^{02915}) and the strongest *ths* allele [*Df(2R)ths238*] (Fig. 5C,F, compare with Fig. 5I). Moreover, the phenotype of *Df(2R)pyr36* was consistently stronger than that of *pyr*^{02915}, suggesting that either *pyr*^{02915} is not a null allele or that *ths* gene function also supports Eve$^+$ cell specification. Although Pyr has the more dominant role, Ths probably also plays a role in supporting Eve expression because the *Df(2R)BSC25* mutant phenotype is more severe than that of *Df(2R)pyr36* mutants. No Eve$^+$ cells are present within the dorsal mesoderm of *Df(2R)BSC25* mutants, a phenotype similar to that of *htl* mutants (Fig. 6B) (Stathopoulos et al., 2004).

To investigate the roles of Pyr and Ths in controlling cell differentiation, which might differ from their roles during cell migration, we focused on how ectopic expression of these ligands affects specification of Eve$^+$ cells within the dorsal mesoderm of the embryo. We have demonstrated previously that when Ths is ectopically expressed in the ectoderm using the *69B*-Gal4 driver, ectopic Eve$^+$ cells result; this is similar to the phenotype observed when constitutively activated Htl is ectopically expressed in the same manner (see Fig. S3E in the supplementary material) (Stathopoulos et al., 2004). We found that ectopic expression of Pyr driven by *69B*-Gal4 also increases the number of Eve$^+$ cells (see Fig. S3D in the supplementary material). Normally, three to four Eve$^+$ cells are specified in 12 hemisegments (see Fig. S3C in the

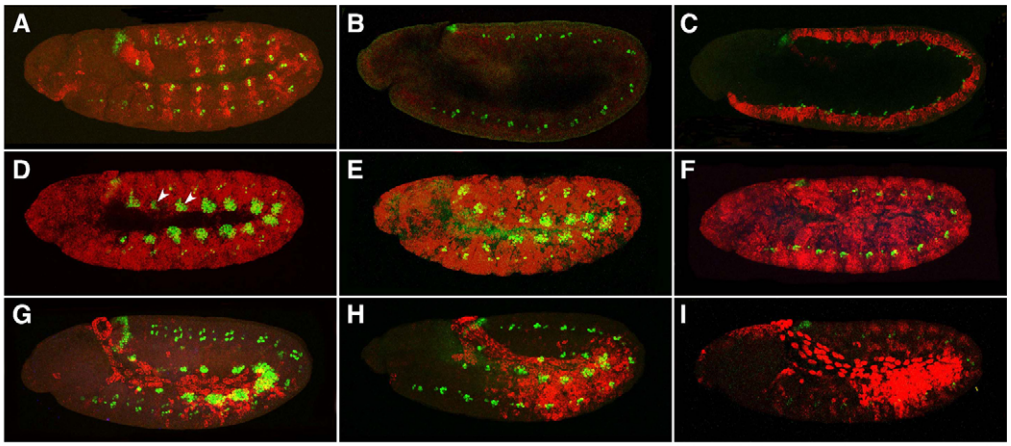

Fig. 6. Pyr and Ths, but not Bnl, can support Htl activation to effect expression of Eve within dorsal mesoderm lineages. *Drosophila* embryos oriented with anterior to the left and dorsal up. Ectopic expression of UAS-*pyr*, UAS-*ths* or UAS-*bnl* in a *Df(2R)BSC25* mutant background, which lacks the endogenous *pyr* and *ths* genes, was achieved using various Gal4 drivers that support expression in different domains of the ectoderm. Depicted are lateral views of stage 11 embryos stained using an anti-Eve antibody (green) and by in situ hybridization with riboprobes to detect *pyr* (D,G), *ths* (A-C,E,H) or *bnl* (F,I) transcript levels (red). (**A**) Endogeneous expression of *ths* in wild-type embryos. Eve$^+$ cells are present in 12 hemisegments. (**B**) *ths* expression in *Df(2R)BSC25* mutant embryos. No dorsal mesoderm-derived Eve$^+$ cells are present. Eve staining is detected only in the central nervous system, expression that is FGF-signaling independent. (**C**) Expression of *ths* in the ventral midline using *sim*-Gal4 does not support expression of Eve in a homozygous *Df(2R)BSC25* mutant background. (**D-F**) Ectopic expression of *pyr* (D) or *ths* (E) in the ectoderm using *69B*-Gal4 does support expression of Eve$^+$ in a homozygous *Df(2R)BSC25* mutant background, whereas *bnl* (F) does not. (**G-I**) Ectopic expression of *pyr* (G) or *ths* (H) in the ectoderm using *zenVRE.Kr*-Gal4 also supports expression of Eve$^+$ in a homozygous *Df(2R)BSC25* mutant background, whereas again *bnl* (I) does not.

supplementary material). In the presence of excess levels of Pyr or Ths, ~6-15 cells were specified and Eve expression was expanded to 14 hemisegments (compare Fig. S3C with Fig. S3D in the supplementary material). When activated Ras is ectopically expressed in the ectoderm, a similar increase in the number of Eve$^+$ cells is observed (Carmena et al., 1998).

Next, we compared the ability of *pyr*, *ths* or *bnl* to rescue Eve$^+$ expression in the *Df(2R)BSC25* mutant background under conditions of equivalent expression. Either Pyr or Ths was able to support Eve$^+$ expression within dorsal mesoderm cells within *Df(2R)BSC25* mutants when expressed using *69B*-Gal4 (‘full rescue’; Fig. 6D,E, compare with Fig. 6B) or *zenVRE.Kr*-Gal4 (‘partial rescue’; Fig. 6G,H, compare with Fig. 6B) drivers. Similar expression of Bnl failed to support the specification of any Eve$^+$ cells (Fig. 6F,I). In addition, when expressed at the ventral midline using *sim*-Gal4, Bnl, Pyr and Ths all failed to support Eve expression (see Fig. 6C; data not shown). In summary, these results suggest that FGF receptors exhibit ligand-binding preferences, and that the ligands must be expressed in proximity to the Htl FGFR for activation to occur.

DISCUSSION

The experiments outlined above demonstrate that the *Drosophila* FGFs Pyr, Ths and Bnl have different functions and that the activation of FGF receptors by specific ligands affects particular biological processes. Examination of an allelic series of *pyr* and *ths* mutants suggests that *pyr* and *ths* are not redundant in function: both influence mesoderm spreading, whereas *pyr* is the dominant player controlling Eve$^+$ cell specification within the dorsal mesoderm (Figs 3 and 5). We have demonstrated previously that ectopic expression of *ths* by *twist*-Gal4 and *69B*-Gal4 in the *Df(2R)BSC25* mutant background can support Htl FGFR activation (Stathopoulos et al., 2004). However, in this study, we assayed whether the expression supported in distinct domains would support Htl activation. By a series of ‘rescue’ experiments, through ectopic expression of one ligand in the *Df(2R)BSC25* mutant background, we obtained evidence that localized expression of the ligands is important for proper mesoderm spreading. We find, surprisingly, that the ligands exhibit differences in their functional range of action (Fig. 4). In addition, using this same approach, we find that either Pyr or Ths can support Eve$^+$ cell specification within the dorsal mesoderm, but that Bnl cannot (Fig. 6). Collectively, these data suggest that the Pyr and Ths FGFs function as ligands for the Htl FGFR and that specificity of FGF-FGFR interactions exists in *Drosophila*.

Specificity of FGFR activation: only three FGF-FGFR combinations function in *Drosophila*

Our results demonstrate that both Pyr and Ths FGF ligands can activate the Htl FGFR, whereas only the Bnl FGF ligand can activate the Btl FGFR (Fig. 6 and see Fig. S2 in the supplementary material). Specificity of FGFR activation was observed: *pyr* or *ths*, but not *bnl*, expression is able to activate Htl to affect expression of Eve, and *bnl*, but neither *pyr* nor *ths*, is able to support tracheal specification. No evidence was obtained that other cross-interactions occur (i.e. Pyr-Btl, Ths-Btl or Bnl-Htl), which demonstrates that Gal4-mediated ectopic expression does not simply ‘swamp the system’. This experimental approach also ‘levels the playing field’, as expression of each ligand is driven at the same time and place and presumably at similar levels. We conclude that only three FGF-FGFR combinations function in *Drosophila* (i.e. Pyr-Htl, Ths-Htl and Bnl-Btl), which supports the idea that FGFRs exhibit ligand-binding preferences. Previous studies have investigated FGF signaling specificity by analyzing the ability of other receptor tyrosine kinases to support cell migration or by activating particular intracellular signaling pathways to examine which are required to effect FGFR-dependent cell migration versus cell differentiation (Dossenbach et al., 2001; Wilson et al., 2005). In this work, we analyzed the specificity of FGF ligand-receptor interactions and how they contribute to particular developmental processes.

Different FGF ligand activities regulate particular developmental processes

When ligand expression is supported by *twist*-Gal4, Htl FGFRs presumably become saturated because dpERK is ectopically activated in all cells and spreading is negatively affected (see Fig. S1 in the supplementary material). One explanation for why this might affect mesoderm cell spreading is that these FGF-saturated

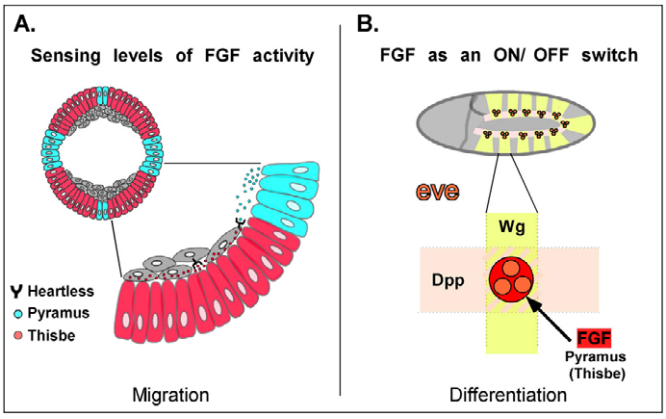

Fig. 7. A model for FGF signaling through Heartless. (**A**) The location of the Ths and Pyr expression domains is important for the proper regulation of mesoderm migration. Both ligands are required, presumably because they have different activities. (**B**) During specification of dorsal mesoderm lineages, including specification of Eve$^+$ cells (orange), FGFs feed into an array of signaling molecules [Wingless (Wg) and Dpp] necessary to specify dorsal mesoderm lineages. We suggest that any FGF ligand (red), expressed in the region of Dpp and Wg overlap and able to activate the respective FGFR, would suffice to support cell differentiation. Wg, Wingless.

mesoderm cells may no longer be competent to respond to endogenous ligands that provide directional cues. Recently, we have shown that movement of the mesoderm cells during gastrulation is in fact directional (McMahon et al., 2008). Pyr and Ths ligands are differentially expressed during gastrulation and this might provide the necessary positional information required to direct migration of the mesoderm (see Fig. 7A).

We propose that Pyr and Ths have different activities that fulfil aspects of FGFR activation required to support cell migration (Fig. 7A). Ectopic expression of Pyr within the ectoderm negatively affects mesoderm spreading (Fig. 1H-M), which suggests that the refined expression domain of *pyr* within cells of the dorsal ectoderm is normally required to guide the mesoderm cells toward dorsal regions. However, even though ectopic expression of *ths* in the ectoderm has no effect on mesoderm spreading, *ths* mutants also exhibit defects in mesoderm spreading, demonstrating that both genes are required, perhaps to control different aspects of the migration. Our 'rescue' experiments using the *zenVRE.Kr*-Gal4 driver support the view that Pyr has a longer functional range than Ths (Fig. 4N,O). These differences in range of function might correlate with different diffusion capabilities, but an alternative explanation is that the ligands activate the receptor with different affinities. Additional experiments will be necessary to distinguish their exact functions and to uncover the molecular basis for the differential functions of Pyr and Ths; we suggest that in vivo imaging and quantitative analysis (McMahon et al., 2008) of single-mutant phenotypes will provide insights.

With regard to the FGF-dependent cell differentiation, our 'rescue' experiments suggest that ectopic expression of either Pyr or Ths is sufficient to support Eve$^+$ cell specification (Fig. 6D,E). The reason why loss of *ths* has less of an effect on Eve$^+$ cell specification is most likely because *pyr* is prominently expressed in the vicinity of the future Eve$^+$ cells; normally, Pyr supports this function, but Ths can support this activity if presented at sufficient levels within the correct domain. Furthermore, we propose that FGF signaling might not play an instructive role in supporting *eve* expression (Fig. 7B). Other signaling pathways already provide positional information required for the specification of Eve$^+$ cells; FGF signaling pathway activation might simply serve a permissive role, and in this context either ligand would suffice.

Conclusion: implications for vertebrate biology?

We have used *Drosophila* to study FGF signaling and determine why multiple ligands are utilized to activate the same receptor. It will be informative to obtain additional insights into how these ligands differ in their activities. The expression domains of the ligands do confer information that is important for controlling developmental processes, but their individual protein sequences also impart differential functionality. For instance, the ligands might exhibit different affinities for specific HSPGs that influence their range of diffusion, or the proteins themselves may have different stabilities. Future experiments will also define the FGF ligand preferences that exist to support FGF signaling at later stages of development.

At least 15 human genetic diseases result from mutations within FGFR genes and each disease is caused by a different mutation shown to affect receptor activation (Chen and Deng, 2005). Several mutations in FGFR lead to an expansion of FGF ligand-binding preference (Ornitz, 2005); however, it is still not clear why different mutations yield different syndromes. Continuing this work in order to understand how different FGF ligands activate the same receptor to effect different outcomes is an important goal, as this may provide insights into why different mutations in the same FGFR lead to various dysplasias and diseases (Wilkie, 2005).

We thank S. Crews, M. Frasch, E. Giniger, M. Krasnow, M. Levine, A. Michelson, the Bloomington Stock Center, and Harvard Exelixis Distribution Center for providing antibodies and fly stocks; Manfred Frasch and the Stathopoulos laboratory members, especially Sarah Payne, for discussions and comments on the manuscript; Leslie Dunipace for conducting the inverse PCR experiments; Smadar Ben-Tabou de-Leon for advice on the qPCR experiments; and Jagan Srinivasan for help with graphical representations. This work was supported by grants to A.S. from the NIH (R01 GM078542), the Searle Scholars Program, and the March of Dimes (Basil O'Conner Starter Scholar Award, 5-FY06-12). Deposited in PMC for release after 12 months.

Supplementary material

Supplementary material for this article is available at
http://dev.biologists.org/cgi/content/full/136/5/739/DC1

References

Ahmad, S. M. and Baker, B. S. (2002). Sex-specific deployment of FGF signaling in Drosophila recruits mesodermal cells into the male genital imaginal disc. *Cell* **109**, 651-661.
Beiman, M., Shilo, B. Z. and Volk, T. (1996). Heartless, a Drosophila FGF receptor homolog, is essential for cell migration and establishment of several mesodermal lineages. *Genes Dev.* **10**, 2993-3002.
Birnbaum, D., Popovici, C. and Roubin, R. (2005). A pair as a minimum: the two fibroblast growth factors of the nematode Caenorhabditis elegans. *Dev. Dyn.* **232**, 247-255.
Carmena, A., Gisselbrecht, S., Harrison, J., Jimenez, F. and Michelson, A. M. (1998). Combinatorial signaling codes for the progressive determination of cell fates in the Drosophila embryonic mesoderm. *Genes Dev.* **12**, 3910-3922.
Chen, L. and Deng, C. X. (2005). Roles of FGF signaling in skeletal development and human genetic diseases. *Front. Biosci.* **10**, 1961-1976.
Coumoul, X. and Deng, C. X. (2003). Roles of FGF receptors in mammalian development and congenital diseases. *Birth Defects Res. C Embryo Today* **69**, 286-304.
Dossenbach, C., Rock, S. and Affolter, M. (2001). Specificity of FGF signaling in cell migration in Drosophila. *Development* **128**, 4563-4572.
Eswarakumar, V. P., Lax, I. and Schlessinger, J. (2005). Cellular signaling by fibroblast growth factor receptors. *Cytokine Growth Factor Rev.* **16**, 139-149.
Frasch, M. (1995). Induction of visceral and cardiac mesoderm by ectodermal Dpp in the early Drosophila embryo. *Nature* **374**, 464-467.

Frasch, M. (1999). Intersecting signalling and transcriptional pathways in Drosophila heart specification. *Semin. Cell Dev. Biol.* **10**, 61-71.
Gabay, L., Seger, R. and Shilo, B. Z. (1997). MAP kinase in situ activation atlas during Drosophila embryogenesis. *Development* **124**, 3535-3541.
Gisselbrecht, S., Skeath, J. B., Doe, C. Q. and Michelson, A. M. (1996). heartless encodes a fibroblast growth factor receptor (DFR1/DFGF-R2) involved in the directional migration of early mesodermal cells in the Drosophila embryo. *Genes Dev.* **10**, 3003-3017.
Gryzik, T. and Muller, H. A. (2004). FGF8-like1 and FGF8-like2 encode putative ligands of the FGF receptor Htl and are required for mesoderm migration in the Drosophila gastrula. *Curr. Biol.* **14**, 659-667.
Huang, P. and Stern, M. J. (2005). FGF signaling in flies and worms: more and more relevant to vertebrate biology. *Cytokine Growth Factor Rev.* **16**, 151-158.
Ishimoto, H., Takahashi, K., Ueda, R. and Tanimura, T. (2005). G-protein gamma subunit 1 is required for sugar reception in Drosophila. *EMBO J.* **24**, 3259-3265.
Kosman, D., Mizutani, C. M., Lemons, D., Cox, W. G., McGinnis, W. and Bier, E. (2004). Multiplex detection of RNA expression in Drosophila embryos. *Science* **305**, 846.
Lehmann, R. and Tautz, D. (1994). In situ hybridization to RNA. *Methods Cell Biol.* **44**, 575-598.
Leptin, M. and Grunewald, B. (1990). Cell shape changes during gastrulation in Drosophila. *Development* **110**, 73-84.
Mariani, F. V., Ahn, C. P. and Martin, G. R. (2008). Genetic evidence that FGFs have an instructive role in limb proximal-distal patterning. *Nature* **453**, 401-405.
McMahon, A., Supatto, W., Fraser, S. E. and Stathopoulos, A. (2008). Dynamic analyses of Drosophila gastrulation provide insights into collective cell migration. *Science* **322**, 1546-1550.
Michelson, A. M., Gisselbrecht, S., Zhou, Y., Baek, K. H. and Buff, E. M. (1998). Dual functions of the heartless fibroblast growth factor receptor in development of the Drosophila embryonic mesoderm. *Dev. Genet.* **22**, 212-229.
Ornitz, D. M. (2005). FGF signaling in the developing endochondral skeleton. *Cytokine Growth Factor Rev.* **16**, 205-213.
Ornitz, D. M. and Itoh, N. (2001). Fibroblast growth factors. *Genome Biol.* **2**, reviews3005.1-3005.12.
Ornitz, D. M., Xu, J., Colvin, J. S., McEwen, D. G., MacArthur, C. A., Coulier, F., Gao, G. and Goldfarb, M. (1996). Receptor specificity of the fibroblast growth factor family. *J. Biol. Chem.* **271**, 15292-15297.
Preston, C. R., Sved, J. A. and Engels, W. R. (1996). Flanking duplications and deletions associated with P-induced male recombination in Drosophila. *Genetics* **144**, 1623-1638.
Rentzsch, F., Fritzenwanker, J. H., Scholz, C. B. and Technau, U. (2008). FGF signalling controls formation of the apical sensory organ in the cnidarian Nematostella vectensis. *Development* **135**, 1761-1769.
Rottinger, E., Saudemont, A., Duboc, V., Besnardeau, L., McClay, D. and Lepage, T. (2008). FGF signals guide migration of mesenchymal cells, control skeletal morphogenesis and regulate gastrulation during sea urchin development. *Development* **135**, 353-365.
San Martin, B. and Bate, M. (2001). Hindgut visceral mesoderm requires an ectodermal template for normal development in Drosophila. *Development* **128**, 233-242.
Sato, M. and Kornberg, T. B. (2002). FGF is an essential mitogen and chemoattractant for the air sacs of the drosophila tracheal system. *Dev. Cell* **3**, 195-207.
Shishido, E., Ono, N., Kojima, T. and Saigo, K. (1997). Requirements of DFR1/Heartless, a mesoderm-specific Drosophila FGF-receptor, for the formation of heart, visceral and somatic muscles, and ensheathing of longitudinal axon tracts in CNS. *Development* **124**, 2119-2128.
Spralding, A. C. and Rubin, G. M. (1982). Genetic transformation of *Drosophila* with transposable element vectors. *Science* **218**, 348-353.
Stathopoulos, A., Tam, B., Ronshaugen, M., Frasch, M. and Levine, M. (2004). pyramus and thisbe: FGF genes that pattern the mesoderm of Drosophila embryos. *Genes Dev.* **18**, 687-699.
Sutherland, D., Samakovlis, C. and Krasnow, M. A. (1996). branchless encodes a Drosophila FGF homolog that controls tracheal cell migration and the pattern of branching. *Cell* **87**, 1091-1101.
Szebenyi, G. and Fallon, J. F. (1999). Fibroblast growth factors as multifunctional signaling factors. *Int. Rev. Cytol.* **185**, 45-106.
Thibault, S. T., Singer, M. A., Miyazaki, W. Y., Milash, B., Dompe, N. A., Singh, C. M., Buchholz, R., Demsky, M., Fawcett, R., Francis-Lang, H. L. et al. (2004). A complementary transposon tool kit for Drosophila melanogaster using P and piggyBac. *Nat. Genet.* **36**, 283-287.
Thisse, B. and Thisse, C. (2005). Functions and regulations of fibroblast growth factor signaling during embryonic development. *Dev. Biol.* **287**, 390-402.
Wilkie, A. O. (2005). Bad bones, absent smell, selfish testes: the pleiotropic consequences of human FGF receptor mutations. *Cytokine Growth Factor Rev.* **16**, 187-203.
Wilson, R., Vogelsang, E. and Leptin, M. (2005). FGF signalling and the mechanism of mesoderm spreading in Drosophila embryos. *Development* **132**, 491-501.
Xiao, H., Hrdlicka, L. A. and Nambu, J. R. (1996). Alternate functions of the single-minded and rhomboid genes in development of the Drosophila ventral neuroectoderm. *Mech. Dev.* **58**, 65-74.
Yang, X., Dormann, D., Munsterberg, A. E. and Weijer, C. J. (2002). Cell movement patterns during gastrulation in the chick are controlled by positive and negative chemotaxis mediated by FGF4 and FGF8. *Dev. Cell* **3**, 425-437.
Zhang, X., Ibrahimi, O. A., Olsen, S. K., Umemori, H., Mohammadi, M. and Ornitz, D. M. (2006). Receptor specificity of the fibroblast growth factor family. The complete mammalian FGF family. *J. Biol. Chem.* **281**, 15694-15700.

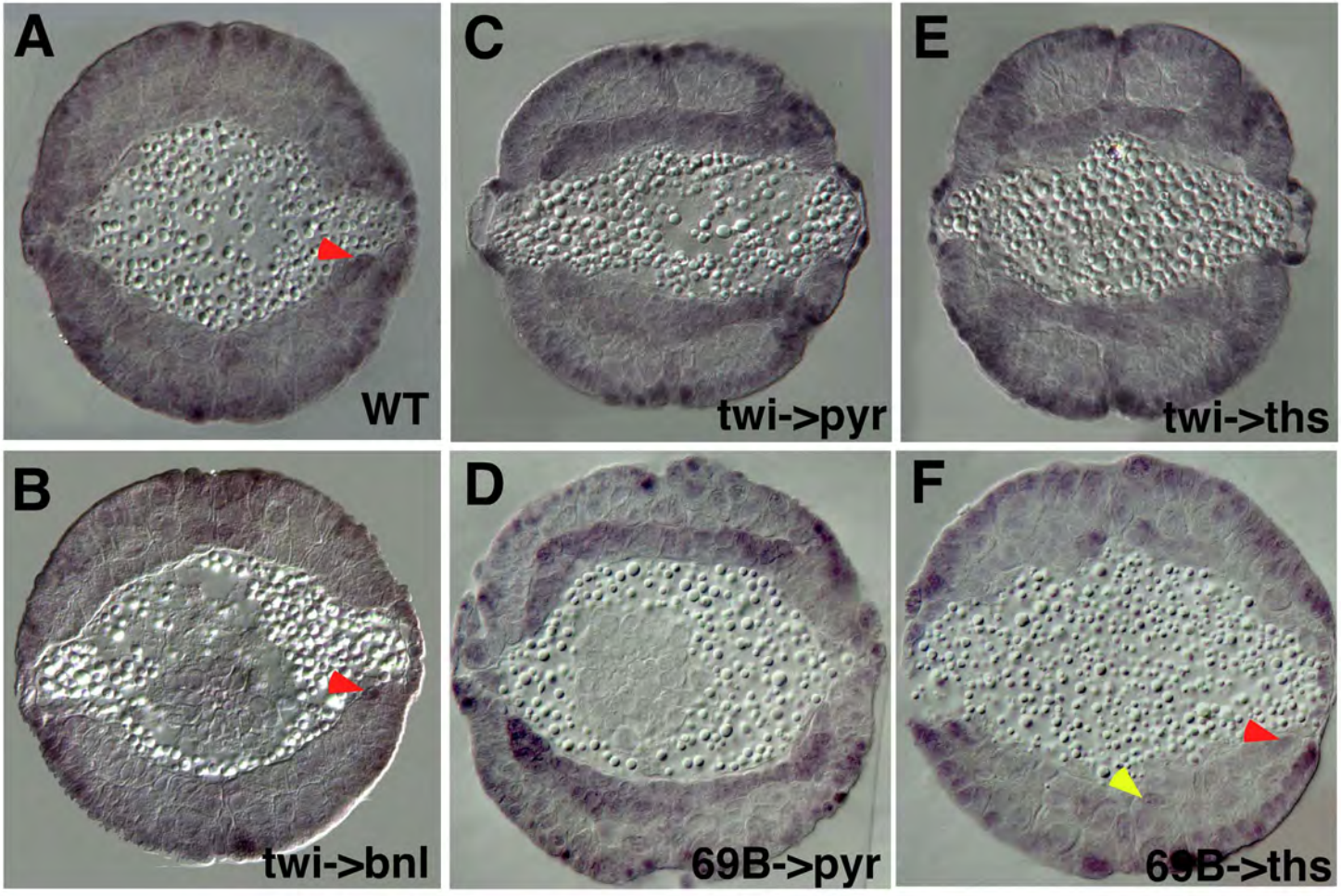
A
WT
C
twi->pyr
E
twi->ths
B
twi->bnl
D
69B->pyr
F
69B->ths

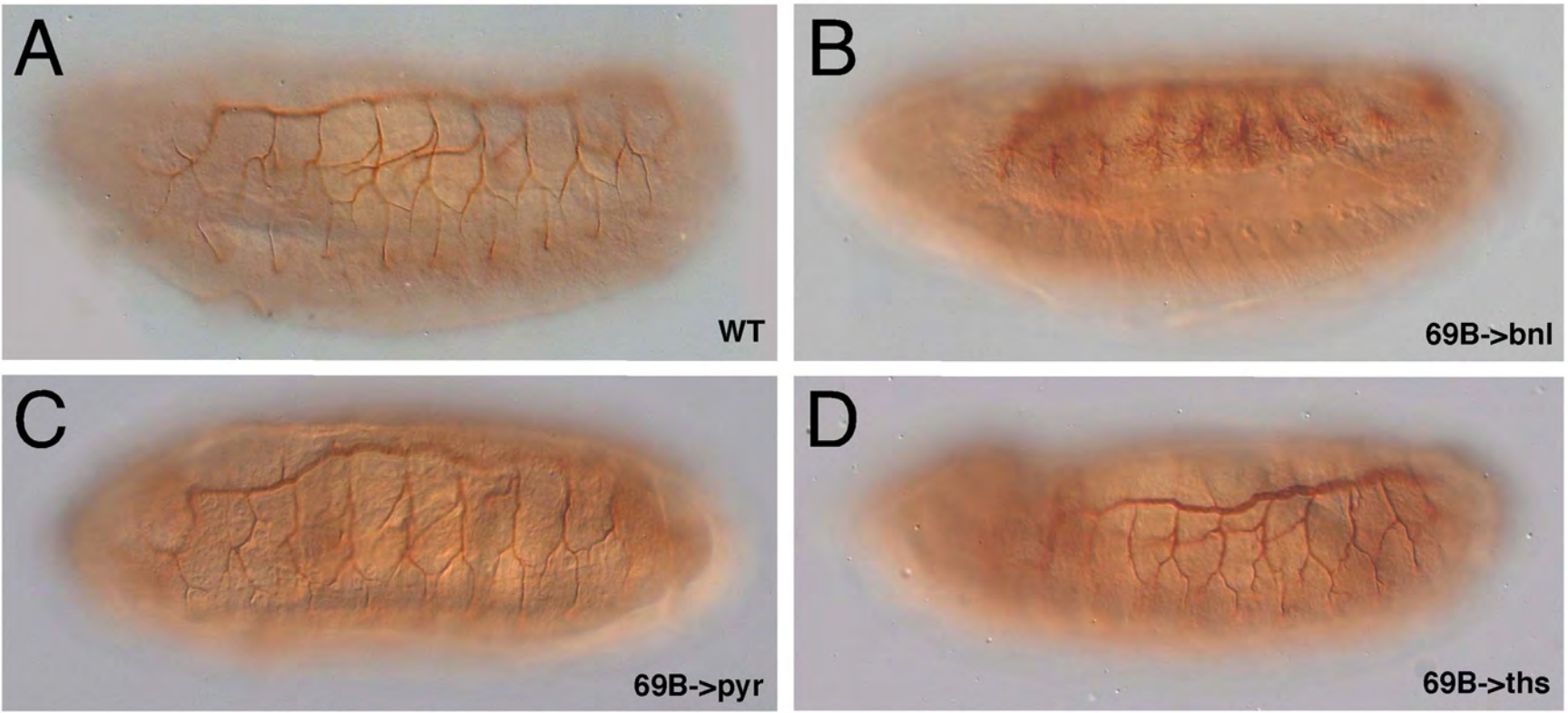
A
WT
B
69B->bnl
C
69B->pyr
D
69B->ths

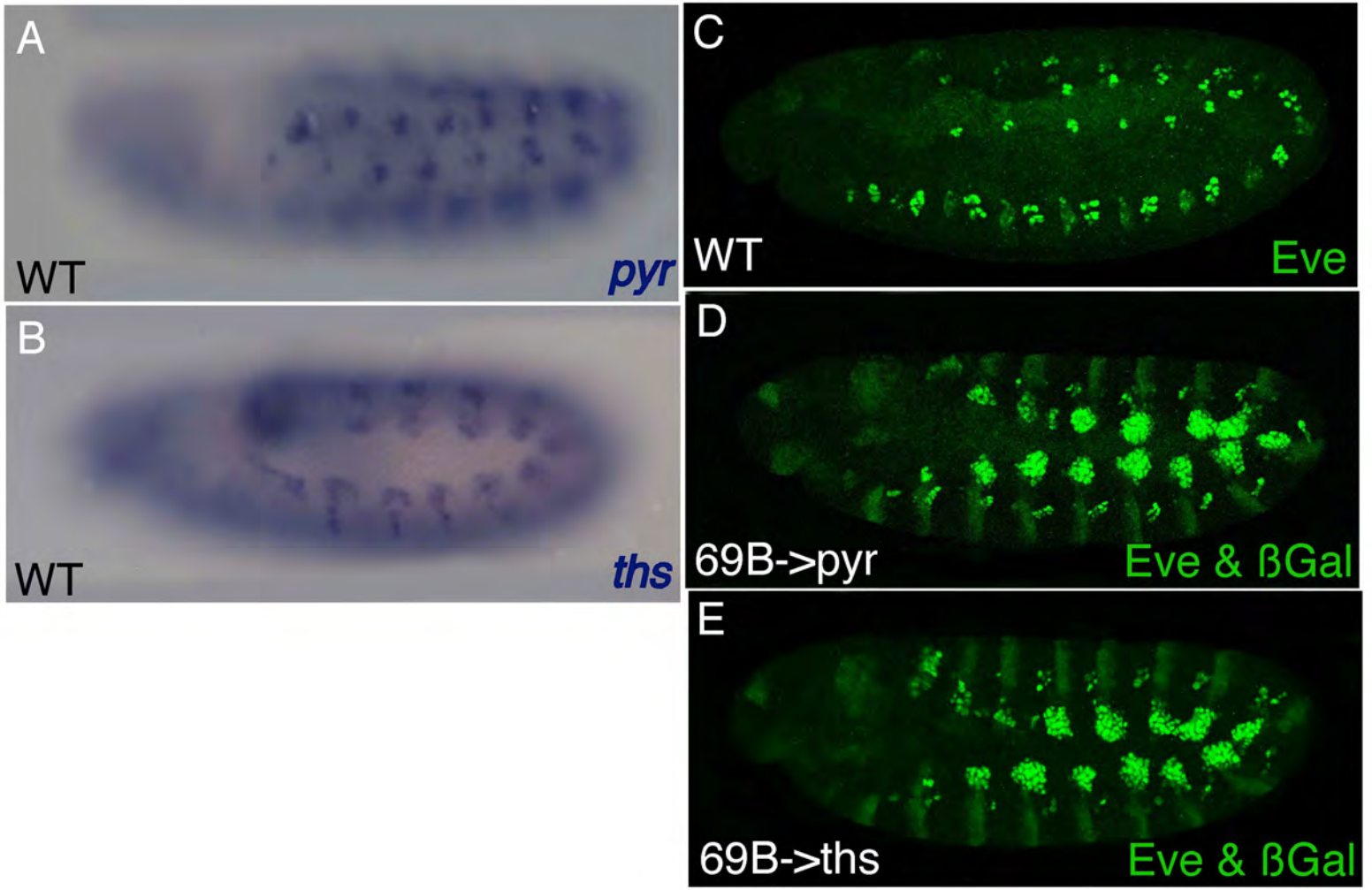
A
WT
pyr
B
WT
ths
C
WT
Eve
D
69B->pyr
Eve & ßGal
E
69B->ths
Eve & ßGal

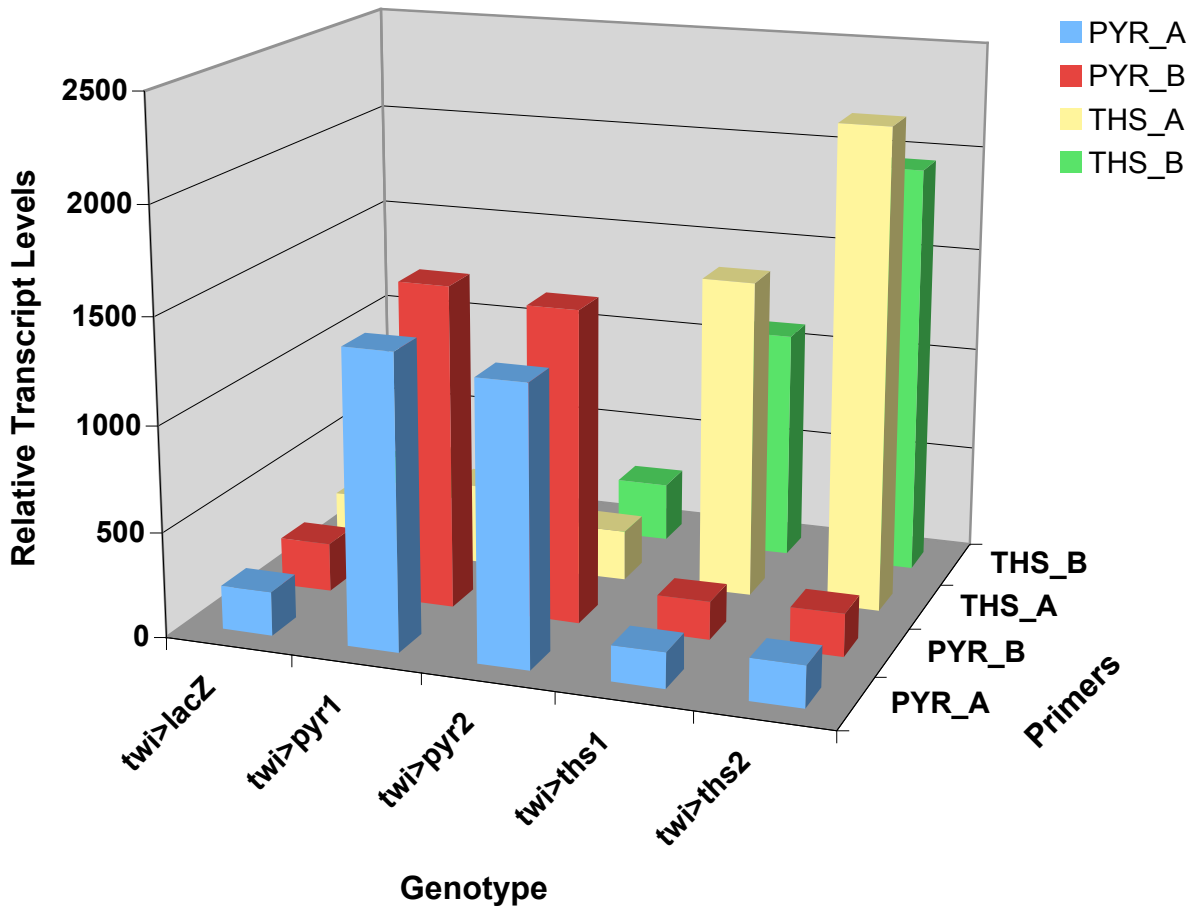

	Number of molecules per primer combination (arbitrary units)				
	twi>lacZ	**twi>pyr1**	**twi>pyr2**	**twi>ths1**	**twi>ths2**
PYR_A	208.51	1392.13	1314.43	168.48	193.21
PYR_B	233.37	1537.62	1480.95	180.82	205.08
THS_A	264.10	382.35	239.38	1510.69	2278.30
THS_B	271.80	403.17	281.27	1099.08	1956.22

Frequency of clumping phenotype in embryos ectopically expressing *pyramus* and *thisbe*

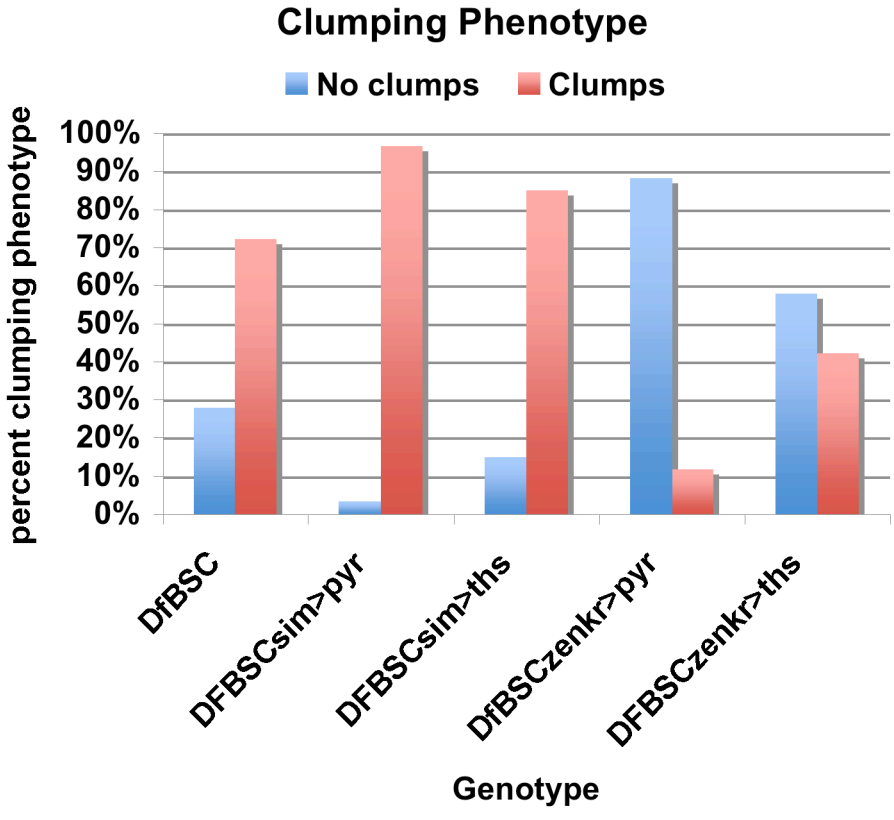

Genotype	Total Number	No clumps	Clumps	p-value
DfBSC25	36	10	26	
DFBSC25,sim>pyr	30	1	29	<0.01
DFBSC25,sim>ths	40	6	34	n.s
DfBSC25,zenVRE.Kr>pyr	17	15	2	< 0.0001
DFBSC25,zenVRE.Kr>ths	19	11	8	n.s

Frequency of multilayed phenotype in embryos ectopically expressing *pyramus* and *thisbe*

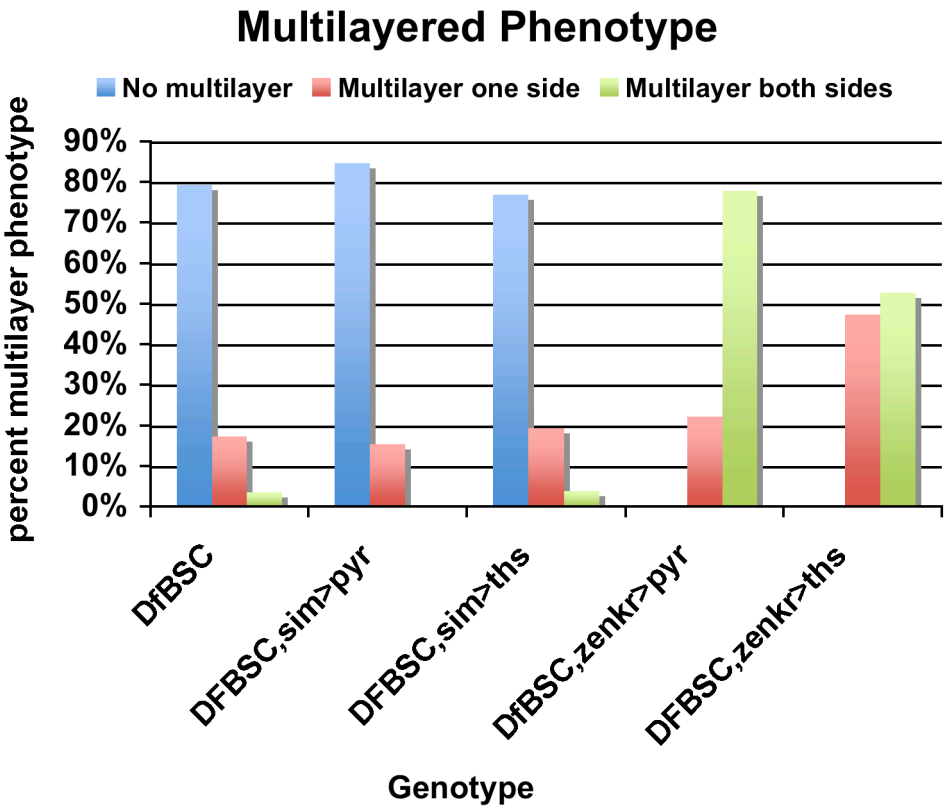

Genotype	No multilayer	Multilayer (one side)	p-value	Multilayer (both sides)	p-value
DfBSC	23	5		1	
DFBSCsim>pyr	22	4	n.s.	0	n.s.
DFBSCsim>ths	20	5	n.s.	1	n.s.
DfBSCzenkr>pyr	0	4	< 0.01	14	< 0.0001
DFBSCzenkr>ths	0	9	< 0.00001	10	< 0.0001